

On hyperlogarithms and Feynman integrals with divergences and many scales

Erik Panzer

*Institutes of Physics and Mathematics, Humboldt-Universität zu Berlin
Unter den Linden 6, 10099 Berlin, Germany*

E-mail: panzer@mathematik.hu-berlin.de

ABSTRACT: Hyperlogarithms provide a tool to carry out Feynman integrals in Schwinger parameters. So far, this method has been applied successfully mostly to finite single-scale processes. However, it can be employed in more general situations.

We give examples of integrations of three- and four-point integrals in Schwinger parameters with non-trivial kinematic dependence, including setups with off-shell external momenta and differently massive internal propagators. The full set of Feynman graphs admissible to parametric integration is not yet understood and we discuss some counterexamples to the crucial property of *linear reducibility*. In special cases we observe how a change of variables can restore this prerequisite for direct integration and thereby enlarge the set of accessible graphs.

Working in dimensional regularization, we furthermore clarify how a simple application of partial integration can be used to convert divergent parametric integrands to convergent ones. In contrast to the subtraction of counterterms, this scheme is ideally suited for our method of integration.

KEYWORDS: multiloop Feynman integrals, dimensional regularization, hyperlogarithms

ARXIV EPRINT: [1401.4361](https://arxiv.org/abs/1401.4361)

Contents

1	Introduction	1
2	Single-scale integrals	3
2.1	Massless propagators	3
2.2	On-shell propagators with one internal mass	4
3	Non-trivial kinematics	5
3.1	Massless on-shell four-point graphs (two scales)	5
3.2	Off-shell massless vertices (three scales)	6
3.3	Conformal four-point integrals	8
3.4	Integrals with massive propagators and up to seven scales	10
3.4.1	Box with two masses and three off-shell legs (seven scales)	11
3.4.2	Box with two adjacent masses and one off-shell leg (five scales)	11
3.4.3	Double-triangle with two legs off-shell (four scales)	12
3.4.4	Double-triangle with two legs off-shell and two masses (six scales)	13
4	Extending linear reducibility	14
4.1	One-loop example: box with two masses vis-à-vis	14
4.2	Three-loop example: K_4	15
5	Divergences in Schwinger parameters	16
5.1	Analytic regularization	17
6	Summary and outlook	19
A	Polynomial reduction and linear reducibility	20
A.1	Hyperlogarithms	21

1 Introduction

Scalar¹ Feynman integrals $\Phi(G)$ associated to a Feynman graph G take the form [3]

$$\Phi(G) = \Gamma(\text{sdd}) \cdot \left[\prod_e \int_0^\infty \frac{\alpha_e^{a_e-1} d\alpha_e}{\Gamma(a_e)} \right] \psi^{\text{sdd}-D/2} \varphi^{-\text{sdd}} \cdot \delta(H) \quad (1.1)$$

¹Products of loop momenta in the numerator (in the momentum space representation) yield the same parametric form [1] (see also section 2.3 of [2]) up to shifted powers of ψ and φ as well as a further polynomial in the numerator. Therefore such *tensor* integrals are included in our discussion throughout.

in Schwinger parameters α_e for each edge $e \in E(G)$ and the power a_e of the corresponding propagator. The graph polynomials [4] are given by sums over all spanning trees T and all spanning two-forests F :

$$\psi = \sum_T \prod_{e \notin T} \alpha_e \quad \text{and} \quad \varphi = \sum_{F=T_1 \cup T_2} q^2(T_1) \prod_{e \notin F} \alpha_e + \psi \sum_e m_e^2 \alpha_e, \quad (1.2)$$

where $q(T_1) := \sum_{v \in T_1} q(v) = -q(T_2)$ denotes the total external momentum entering the tree T_1 and m_e the mass of the internal propagator associated to e .

The Dirac distribution $\delta(H)$ in (1.1) projects on an arbitrary² hyperplane $\{H = 0\}$ which we will always choose as $H = 1 - \alpha_e$ for some fixed edge e . Denoting the number of loops of G by $|G|$, in D dimensions we declare the superficial degree of divergence as

$$\text{sdd} = \sum_e a_e - \frac{D}{2} |G|. \quad (1.3)$$

Our strategy is to successively integrate out Schwinger parameters $\alpha_{e_1}, \alpha_{e_2}, \dots$ in (1.1) following the method of [5] which we implemented in the computer algebra system MapleTM [6]. To compute regulated integrals (e.g. $D = 4 - 2\varepsilon$), we perform the ε -expansion on the integrand of (1.1) and integrate out each term individually.

This approach requires a convergent integral representation of each term in the expansion, but the immediate form (1.1) often turns out to be divergent at the expansion point (e.g. $\varepsilon = 0$). In particular this is always the case whenever G contains (infrared or ultraviolet) sub divergences. In section 5 we derive a systematic procedure to generate different (but equivalent) parametric integral representations with increased domains of convergence, therefore extending the method of parametric integration to arbitrarily divergent ε -expansions.

As a consequence, the earlier results for finite single-scale propagator graphs recalled in section 2 generalize to the divergent cases.

Parametric integration can only be applied to *linearly reducible* graphs G , a criterion on the graph polynomials $S_0 := \{\psi, \varphi\}$ which we recall in appendix A. The idea is that starting from the integrand f_0 of (1.1), for any ordering e_1, \dots, e_N of edges we can find sets $S_n \in \mathbb{Q}[\alpha_{n+1}, \dots, \alpha_N]$ of polynomials that describe the possible singularities of the partial Feynman integrals $f_{n+1} := \int_0^\infty f_n d\alpha_{n+1}$. If each element of S_n is linear in α_{n+1} , the algorithm of [5] can be applied to compute f_{n+1} in terms of hyperlogarithms. These are special classes of multiple polylogarithms and all explicit results in this article will be given in the notation we fix in A.1. There we also explain how the final set S_N of this polynomial reduction constrains the symbol of the Feynman integral $f_{N-1}|_{\alpha_N=1} = \Phi(G)$.

The main section 3 is a collection of examples of integrals with non-trivial dependence on kinematic invariants $\Theta = \{m_e^2, q^2(T), \dots\}$ that are linearly reducible and can thus be integrated parametrically. For illustration we supply explicit new results for selected cases, most of which are (due to their volume) not printed but contained in the attached text file only. Further results might be obtained from the author upon request.

²This freedom of choice is a consequence of (1.1) being a projective integral.

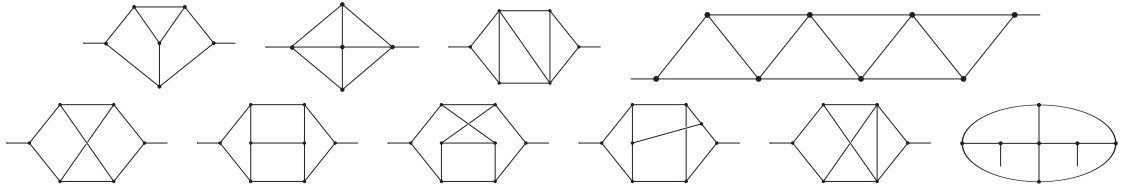


Figure 1. Examples of massless propagators of vertex-width three (first row) and vertex-width four (second row).

We also point out counterexamples to linear reducibility and show in section 4 that in special cases, changes of variables can allow for parametric integration in spite of the graph not being linearly reducible in the original Schwinger parameters.

Acknowledgments

I like to thank Christoph Meyer for pointing out to me the importance of graphs with two different internal masses for the NNLO-computation of single top-quark production and checking some analytic results numerically. Bas Tausk provided invaluable help in hinting me to numerous references on selected integrals. Furthermore I enjoyed interesting discussions with Johannes Henn who motivated me to investigate integrals with divergences and non-trivial kinematics. He also supplied a series of analytic results that helped me to verify my program. Oliver Schnetz explained to me the importance of graphical functions, kindly supplied a list of these and suggested their study in a parametric representation. Finally I like to thank Christian Bogner for many insights into the structure of iterated integrals of many variables and introducing to me the program [7] for sector decomposition that was used for some numeric checks in this article. His completely independent program following [8] provided valuable cross-checks of my own implementation.

2 Single-scale integrals

Before studying more complicated examples, let us briefly review integrals with a single scale: φ depends only on a single kinematic invariant $\{s\} = \Theta$ (a mass or external momentum squared) which therefore factors out completely from (1.1) as $s^{-\text{sdd}}$.

2.1 Massless propagators

The case of massless graphs G with two external legs (depending on their momenta $\pm p$ through $s = p^2$) is so far the only setup where a non-trivial infinite family of linearly reducible graphs is known to exist by

Theorem 2.1 (positive matrix graphs [9]). *All massless vacuum (no external momenta) graphs G of vertex-width $\text{vw}(G) \leq 3$ are linearly reducible and their ε -expansions are \mathbb{Q} -linear combinations of multiple zeta values ζ_{n_1, \dots, n_r} where $n_1, \dots, n_r \in \mathbb{N}$ and $n_r > 1$.*

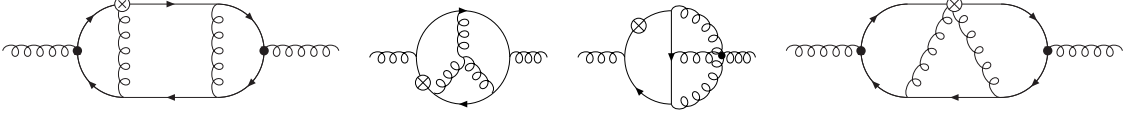


Figure 2. Linearly reducible topologies with one internal mass (fermion lines) and otherwise massless propagators (including the external momentum $p^2 = 0$) from [11–13]. The marked vertex represents an operator insertion, its precise form is irrelevant for the polynomial reduction. Note however that the authors aimed for generating functions of all Mellin moments, and then linear reducibility strongly depends on the form of operator.

Here $\text{vw}(G) \leq 3$ means that we can order the edges e_1, \dots, e_N of G such that for all $1 \leq n \leq N$, there are at most three vertices of G that touch edges in $\{e_1, \dots, e_n\}$ and $\{e_{n+1}, \dots, e_N\}$ at the same time. Even though this is a strong³ constraint on G , we like to stress that it holds for infinitely many non-trivial graphs, all of which thus being proven to evaluate to multiple zeta values. This theorem extends to massless propagators by glueing the external legs to form a vacuum graph. Examples are shown in figure 1.

Starting at three-loops, graphs with $\text{vw}(G) > 3$ occur (e.g. the second row in the figure) and are therefore not covered by theorem 2.1, but we still have

Theorem 2.2 (vacuum graphs with four or five loops [10]). *All massless propagators up to four loops are linearly reducible. Their ε -expansions are \mathbb{Q} -linear combinations of alternating Euler sums $\text{Li}_{n_1, \dots, n_r}(\sigma_1, \dots, \sigma_r)$ where $n_i \in \mathbb{N}$, $\sigma_i^2 = 1$ and $(n_r, \sigma_r) \neq (1, 1)$.*

Remark 2.3. *In [10] we carefully stated this result only for convergent ε -expansions, while the influence of sub divergences on the periods was left unclear. Taking section 5 into account, we now realize that it holds in full generality and applies to arbitrary dimension $D = D_0 - 2\varepsilon$ ($D_0 \in 2\mathbb{N}$) and propagator powers $a_e = n_e + \varepsilon \nu_e$ with $n_e \in \mathbb{Z}$; unaffected by sub divergences (that lead to higher order ε -poles).*

The first counter-examples to linear reducibility of massless propagators appear at five loops and some are discussed in section twelve of [9].

2.2 On-shell propagators with one internal mass

Another one-scale kinematic setup is given by propagator graphs with light-like external momentum $p^2 = 0$ but one internal mass m . In this case, the second graph polynomial

$$\varphi = m^2 \cdot \psi \cdot \sum_{m_e=m} \alpha_e \quad (2.1)$$

splits into polynomials which are themselves linear in each variable, while in general φ is irreducible and quadratic in each α_e for which $m_e \neq 0$ by (1.2). This explains the good linear reducibility despite the presence of many massive edges which was observed in

Theorem 2.4 ([11–13]). *The on-shell ($p^2 = 0$) propagators with equally massive internal fermions (and massless gluons) shown in figure 2 are linearly reducible.*

Parametric integration was successfully employed in these works to obtain all Mellin-moments of specific operator insertions.

³For example, $\text{vw}(G) \leq 3$ implies planarity of G .

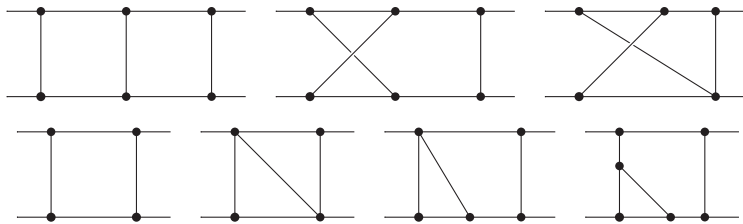


Figure 3. Two-loop four-point functions of theorem 3.1 without one-scale subgraphs.

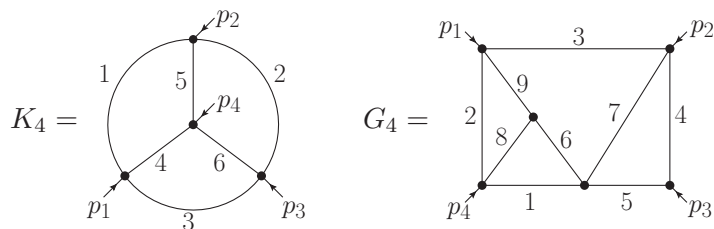


Figure 4. Massless on-shell four-point graphs: While G_4 is linearly reducible (example 3.2), K_4 is not and makes a change of variables necessary (section 4.2).

3 Non-trivial kinematics

With increasing number of kinematic invariants, we expect more complicated Feynman integrals and indeed observe in the following a breakdown of linear reducibility at much lower loop orders. Since all reducible graphs evaluate to polylogarithms, known instances like [14, 15] of elliptic integrals appearing already at two loops are outside the scope of our investigation.

Thus a priori we are restricting ourselves to functions expressible in terms of polylogarithms (with arguments that are algebraic functions of the invariants), and we shall see that not even all of these are linearly reducible in Schwinger parameters.

3.1 Massless on-shell four-point graphs (two scales)

The following result obtained in [16] has so far been the only systematic study of linear reducibility for non-trivial kinematics:

Theorem 3.1. *All massless four-point on-shell graphs ($p_1^2 = p_2^2 = p_3^2 = p_4^2 = 0$) with at most two loops are linearly reducible. In particular these include those of figure 3.*

This result was expected since these functions were known to evaluate to polylogarithms (even with one leg off-shell [17]). At three loops, counter examples to linear reducibility exist [16] like the complete graph K_4 of figure 4 which was recently evaluated in $D = 4 - 2\varepsilon$ and $a_1 = \dots a_6 = 1$ to polylogarithms in [18] using the technique of differential equations. This proves that a failure of linear reducibility in Schwinger parameters does not prohibit a polylogarithmic result. In fact, section 4.2 shows how K_4 can be integrated parametrically nonetheless.

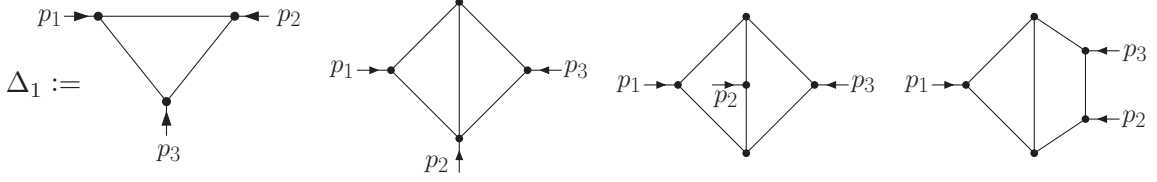


Figure 5. All massless three-point graphs with one or two loops and without one-scale subgraphs (massless propagator insertions). Results are given in [22].

While at three loops all planar massless on-shell four-point functions were calculated in [19] and the non-planar ones are in progress [18], results at four loops seem to be very rare. From our above observations it seems plausible that at least some of them are linearly reducible.

Example 3.2. *The linearly reducible graph G_4 of figure 4 can be integrated in Schwinger parameters along the sequence 1, 2, 8, 6, 9, 7, 5, 4 of edges (setting $\alpha_3 = 1$). The final set of polynomials $S_9 = \{s + u\}$ in the reduction proves that all coefficients f_n of the ε -expansion*

$$\Phi(G_4) = \frac{\Gamma(1 + 4\varepsilon)}{s^{1+4\varepsilon}} \sum_{n=-1}^{\infty} f_n \left(\frac{s}{u} \right) \cdot \varepsilon^n \quad \text{where } s = (p_1 + p_2)^2, u = (p_1 + p_4)^2 \quad (3.1)$$

are harmonic polylogarithms $f_n \in L(\{0, -1\})$ of $x := \frac{s}{u}$. These are special hyperlogarithms introduced in [20] and abbreviated $H_{n_1, \dots, n_r} := L_{\underline{n}_1, \dots, \underline{n}_r}(x)$ for indices representing words $\underline{0} := \omega_0$ and $\pm n := \mp \omega_0^{|\underline{n}|-1} \omega_{\pm 1}$, e.g. $H_{-2} = L_{\omega_0 \omega_{-1}}(x) = \text{Li}_2(-x)$. Explicitly we computed

$$\begin{aligned} f_{-1} = & -\frac{79}{70} \zeta_2^3 H_{-1} - \zeta_3 (15 \zeta_2 H_{-1, -1} - 9 \zeta_2 H_{-1, 0} - H_{-1, -2, -1} + H_{-1, -1, -2} + 6 H_{-1, -1, 0, 0}) \\ & - 6 \zeta_3^2 H_{-1} - \frac{3}{2} \zeta_5 (11 H_{-1, -1} - 5 H_{-1, 0}) - \frac{3}{10} \zeta_2^2 (H_{-1, -2} - 17 H_{-1, -1, 0} - 10 H_{-1, -1, -1}) \\ & - \zeta_2 (H_{-1, -2, 0, 0} - 2 H_{-1, -1, -2, 0} + 3 H_{-1, -1, -2, -1} - H_{-1, -1, -1, 0, 0} + 6 H_{-1, -1, -3} \\ & \quad - 3 H_{-1, -2, -1, -1} - 2 H_{-1, -1, 0, 0, 0}) + H_{-1, -2, -1, 0, 0, 0} - H_{-1, -1, -2, -1, 0, 0} \\ & + H_{-1, -1, -2, 0, 0, 0} - 2 H_{-1, -1, -3, 0, 0} + H_{-1, -2, -1, -1, 0, 0} \end{aligned} \quad (3.2)$$

while we provide f_0 in the attached file. With FIESTA [21] we obtained the approximation

$$\frac{\Phi(G_4)}{\Gamma(1 + 4\varepsilon)} \approx -219.35 \varepsilon^{-1} - 3626.82 + \mathcal{O}(\varepsilon) \quad \text{at } (s, u) = (s_0, u_0) := \left(\frac{1}{2}, \frac{1}{5} \right) \quad (3.3)$$

which serves a successful independent check of our analytic result since it produces the (exact) first digits $-219.4440 \dots \varepsilon^{-1} - 3630.1071 \dots + \mathcal{O}(\varepsilon)$ at (s_0, u_0) .

3.2 Off-shell massless vertices (three scales)

Let us consider graphs with massless internal propagators ($m_e = 0$) and three external momenta as shown in figure 5. At two loops their linear reducibility was observed in [22] and by integration of Schwinger parameters explicit results up to weight four were obtained.

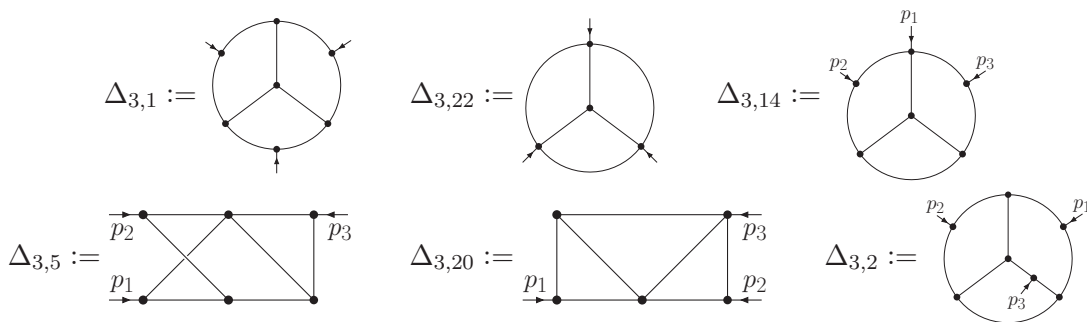


Figure 6. These three-loop three-point graphs are discussed in example 3.5.

These are most conveniently expressed in terms of auxiliary complex⁴ variables z, \bar{z} such that the square-root of the Källén function λ becomes rational:

$$p_2^2 = p_1^2 \cdot z\bar{z} \quad \text{and} \quad p_3^2 = p_1^2 \cdot (1-z)(1-\bar{z}), \quad \text{such that} \quad (3.4)$$

$$(z - \bar{z})^2 = \lambda := p_1^2 + p_2^2 + p_3^2 - 2p_1p_2 - 2p_1p_3 - 2p_2p_3.$$

Example 3.3. The triangle Δ_1 expands near $D = 4 - 2\varepsilon$ with $a_1 = a_2 = a_3 = 1$ as

$$\Phi(\Delta_1) = \frac{\Gamma(1+\varepsilon)}{z-\bar{z}} \cdot p_1^{-2(1+\varepsilon)} \cdot \sum_{n=0}^{\infty} f_n(z, \bar{z}) \varepsilon^n \quad \text{with the leading order given by}$$

$$f_0 = 4i\Im \{ \text{Li}_2(z) + \ln|z| \cdot \ln(1-z) \}, \quad \text{the Bloch-Wigner dilogarithm.}$$

Up to two loops, the functions (like f_n in example 3.3) occurring in the ε -expansions have symbols with letters drawn from the alphabet $\Sigma_\Delta := \{z, \bar{z}, 1-z, 1-\bar{z}, z-\bar{z}\}$. These were first studied in [22] and generalize the single-valued multiple polylogarithms of [23]. Running the polynomial reduction algorithm proved

Theorem 3.4. All massless three-point graphs with up to three loops (some examples are depicted in figure 6) are linearly reducible.

The final sets S_N of the polynomial reduction provide the alphabets of the symbols. We found that these always contain the set Σ_Δ familiar from two loops, but in some cases also the additional letters $z\bar{z} - 1$, $z + \bar{z} - 1$ and $z\bar{z} - z - \bar{z}$ occur.

We computed these functions in $D = 4 - 2\varepsilon$ dimensions with unity propagator powers $a_e = 1$ for all edges $e \in E$ and performed checks exploiting symmetry properties, known results in single-scale limits and numeric evaluations. However, the length of the results and the rich structure of the occurring polylogarithms suggests a detailed and separate discussion elsewhere. We provide some selected data for the graphs of figure 6 in

⁴The Euclidean region $p_1^2, p_2^2, p_3^2 > 0$ corresponds to positive values of $z\bar{z}$ and $(1-z)(1-\bar{z})$. This means either complex conjugate $\bar{z} = z^*$ (when $\lambda < 0$) or independent real $z, \bar{z} \in \mathbb{R}$ (when $\lambda > 0$); cf. [22].

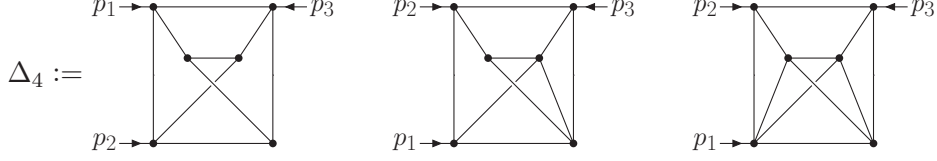


Figure 7. Examples of linearly reducible massless vertices with more than three loops.

Example 3.5. *Three-point functions can have very different complexity: The simplest examples of figure 6 evaluate in leading order to rational functions like*

$$\Phi(\Delta_{3,1}) = \frac{20\zeta_5}{p_1^2 p_2^2 p_3^2} + \mathcal{O}(\varepsilon) \quad \Phi(\Delta_{3,14}) = -\frac{2\zeta_3}{p_2^2 p_3^2 \varepsilon} + \mathcal{O}(\varepsilon^0) \quad \Phi(\Delta_{3,22}) = \frac{2\zeta_3}{\varepsilon} + \mathcal{O}(\varepsilon^0), \quad (3.5)$$

or to hyperlogarithms $L_w := L_w(z)$ and $\bar{L}_w := L_{w'}(\bar{z})$ with $w, w' \in \{0, 1\}^\times$ not involving the symbol letter $z - \bar{z}$ (these are called *SVMP* in [24] or *SVHPL* in [25]), e.g.

$$\begin{aligned} \Phi(\Delta_{3,20}) = & \frac{p_1^{-2}}{z - \bar{z}} \left\{ \zeta_3 \left(4\bar{L}_{0,1,1} - 4L_{0,1,1} + 6L_{0,1}\bar{L}_0 - 6L_0\bar{L}_{0,1} - 6\bar{L}_{0,1,0} + 6L_{0,1,0} \right) \right. \\ & + L_{0,1,1,0,1,0} - \bar{L}_{0,1,1,0,1,0} + \bar{L}_{0,1,0,1,1,0} - L_{0,1,0,1,1,0} + L_{0,1,1}\bar{L}_{0,1,0} - L_{0,1,0}\bar{L}_{0,1,1} \\ & + L_0\bar{L}_{0,1,0,1,1} - L_{0,1,0,1,1}\bar{L}_0 + L_{0,1,1,0,1}\bar{L}_0 - L_0\bar{L}_{0,1,1,0,1} \\ & \left. + L_{0,1}\bar{L}_{0,1,0,1} - L_{0,1,0,1}\bar{L}_{0,1} + L_{0,1,1,0}\bar{L}_{0,1} - L_{0,1}\bar{L}_{0,1,1,0} \right\} + \mathcal{O}(\varepsilon). \quad (3.6) \end{aligned}$$

In contrast, already the leading order of $\Phi(\Delta_{3,2})$ needs the letter $z - \bar{z}$ and the subleading contribution to $\Phi(\Delta_{3,5})$ further employs $z\bar{z} - 1$ and has 2348 different terms $L_w \cdot \bar{L}_{w'}$. These expansions, including $\Phi(\Delta_{3,22})$ up to order ε^3 , can be found in the ancillary file.

Let us stress that linear reducibility of course is retained upon specializing $p_i^2 = 0$ to be light-like for one or two of the external momenta, corresponding to (possibly singular) limits $z \rightarrow 0, 1, \infty$. In particular, combining the remarks of section 5 with theorem 3.4 implies that all three-loop *form-factor integrals* as studied for example in [26, 27] can be integrated parametrically.

Regarding the quickly growing number of graphs at even higher loop orders, but also from a purely conceptual viewpoint, a combinatorial criterion (in the spirit of theorem 2.1) on a three-point graph that at least suffices to deduce linear reducibility (without the need of running the polynomial reduction algorithm) in some cases is highly desirable and in progress. For now let us only remark that reducible graphs also exist at higher loop orders.

Example 3.6. *The non-planar four-loop three-point graph Δ_4 of figure 7 is linearly reducible, its leading order contribution in $D = 4 - 2\varepsilon$ is supplied in the attached file and has a symbol with letters Σ_Δ .*

3.3 Conformal four-point integrals

The same type of functions that describe off-shell three-point graphs was studied as *graphical functions* in [24] and occurs in conformally invariant four-point position-space integrals

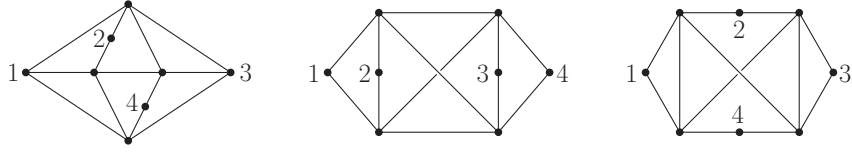


Figure 8. Conformal four-point graphs (with fixed positions x_1, \dots, x_4 at the vertices marked 1 through 4) that are not linearly reducible.

in exactly $D = 4$ dimensions, see [25] and references therein. Namely, conformal invariance implies that functions like the *hard integral*⁵ (dashed edges encode propagators in the numerator)

$$H_{12;34} = \int_{\mathbb{R}^{12}} \frac{d^4 x_5 d^4 x_6 d^4 x_7 \cdot x_{57}^2}{(x_{15}^2 x_{25}^2 x_{35}^2 x_{45}^2) x_{56}^2 (x_{36}^2 x_{46}^2) x_{67}^2 (x_{17}^2 x_{27}^2 x_{37}^2 x_{47}^2)}$$

are a product of a rational prefactor and a function depending only on two conformal cross-ratios which can be parametrized in terms of auxiliary variables z, \bar{z} as

$$z\bar{z} = \frac{x_{12}^2 x_{34}^2}{x_{13}^2 x_{24}^2} \quad \text{and} \quad (1-z)(1-\bar{z}) = \frac{x_{14}^2 x_{23}^2}{x_{13}^2 x_{24}^2}. \quad (3.7)$$

The Schwinger trick delivers a parametric representation for this type of integrals and we found linear reducibility for all such functions at three loops⁶ we considered, for example we integrated $H_{12;34}$ and verified the result that was given in [25]. Furthermore, at four loops without inverse (numerator) propagators, all but the three graphical functions in figure 8 are linearly reducible and can thus be integrated parametrically.

Example 3.7. *The four-point functions depicted in figure 9 are*

$$F_{8,10} = \frac{f_{8,10}}{x_{34}^2 x_{13}^4 x_{24}^4} \quad F_{8,13} = \frac{f_{8,13}}{x_{34}^2 x_{13}^4 x_{24}^4} \quad F_{8,16} = \frac{f_{8,16}}{x_{13}^4 x_{24}^4} \quad (3.8)$$

for polylogarithms $f_{8,10}, f_{8,13}$ and $f_{8,16}$ provided in the accompanying file. These are of homogeneous weight and feature a common denominator summarized in table 1. The last column counts the summands $L_w(z) \cdot L_u(\bar{z})$ of $f_{8,i}$ with non-zero coefficient in the basis where $u \in \{0, 1\}^\times$ while $w \in (\{0, 1\} \cup \Sigma_i)^\times$ can have additional letters $\Sigma_i \subseteq \{\bar{z}, \frac{1}{\bar{z}}, 1 - \bar{z}\}$ given by the zeros of the additional letters of the symbol.

Rough numeric estimates $f_{8,10} \approx 113$, $f_{8,13} \approx 153$ and $f_{8,16} \approx 552$ at $z = \frac{1}{4}$, $\bar{z} = \frac{1}{2}$ obtained by FIESTA provide a successful check of these exact analytic results ($f_{8,10} = 113.579\dots$, $f_{8,13} = 154.160\dots$ and $f_{8,16} = 555.438\dots$).

⁵This is introduced in [25]; $x_{ij} := |x_i - x_j|$ denotes Euclidean distances between vectors $x_i, x_j \in \mathbb{R}^4$.

⁶In this position-space setting one counts the number of internal vertices as “loops” because these are integrated over.

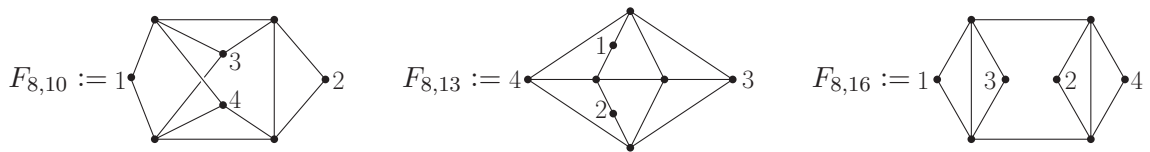


Figure 9. Linearly reducible graphical functions at four loops of varying complexity from example 3.7.

function	denominator	weight	additional symbol letters	number of terms
$f_{8,10}$	$(z - \bar{z})(z + \bar{z} - 2)$	8	$\{z - \bar{z}, z\bar{z} - 1, z + \bar{z} - 1\}$	4235
$f_{8,13}$	$(z - \bar{z})^2$	8	\emptyset	107
$f_{8,16}$	$z\bar{z}(z - \bar{z})$	7	$\{z - \bar{z}\}$	146

Table 1. Details on the conformal integrals of example 3.7 (figure 9).

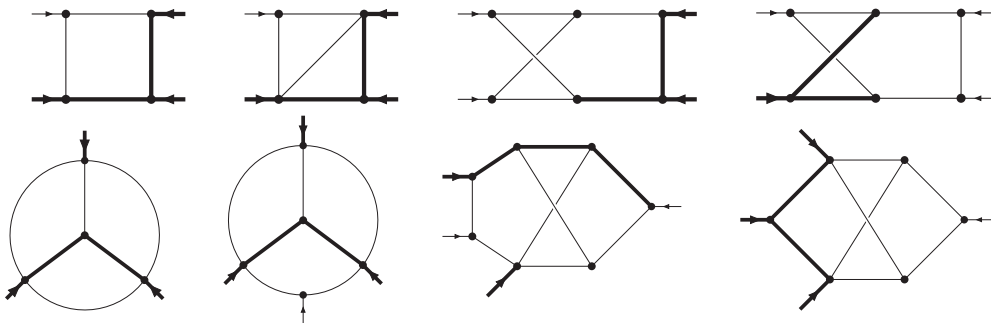


Figure 10. Linearly reducible graphs with some massive (thick edges) and otherwise massless propagators (thin edges). Thin external legs are light-like ($p_i^2 = 0$), while thick external legs may take arbitrary values of p_i^2 .

3.4 Integrals with massive propagators and up to seven scales

Recently, the method of differential equations was employed to obtain analytic results in terms of polylogarithms for a variety of two-loop integrals involving three scales as for example in [28–30]. Clearly it is an interesting question to investigate whether these are linearly reducible; violations of this criterion mean that parametric integration is not possible straight away and might therefore yield to insights how to extend the method as we comment on in section 4.

Thinking in the other direction, even though most Feynman graphs with general kinematics are *not* linearly reducible, figure 10 shows some highly non-trivial integrals we found that are linearly reducible and thus amenable to direct integration. These involve up to three off-shell external momenta and an example with three (different) internal masses.

As a proof of concept we give explicit results for the first two graphs of figure 10 valid in $D = 4 - 2\epsilon$ dimensions with propagator powers $a_e = 1$ for all edges e and Euclidean

scalar products $p^2 \geq 0$ of momenta.

3.4.1 Box with two masses and three off-shell legs (seven scales)

The one-loop box with four external momenta and $p_2^2 = m_1 = m_2 = 0$,

$$\Phi \left(\begin{array}{c} \overrightarrow{p_2} \text{---} \bullet \text{---} \overrightarrow{p_3} \\ | \quad | \\ \bullet \text{---} \overrightarrow{p_1} \text{---} \bullet \text{---} \overrightarrow{p_4} \end{array} \right) = \frac{\Gamma(2 + \varepsilon)}{m_4^{4+2\varepsilon}} \cdot \sum_{n=-1}^{\infty} f_n \left(\frac{m_3^2}{m_4^2}, \frac{p_1^2}{m_4^2}, \frac{p_3^2}{m_4^2}, \frac{p_4^2}{m_4^2}, \frac{(p_1 + p_2)^2}{m_4^2}, \frac{(p_1 + p_4)^2}{m_4^2} \right) \varepsilon^n \quad (3.9)$$

is linearly reducible (the first graph in figure 10) and can therefore be integrated in Schwinger parameters. The arguments of the polylogarithms f_n in general involve several square-roots of rational functions of the six dimensionless ratios, which can be rationalized by quadratic transformations similar to (3.4). For brevity we thus specialize to simpler kinematics in the sequel.

3.4.2 Box with two adjacent masses and one off-shell leg (five scales)

Restricting to $p_3^2 = p_4^2 = 0$, define the dimensionless ratios

$$p := \frac{p_1^2}{m_4^2}, \quad m := \frac{m_3^2}{m_4^2}, \quad s := \frac{(p_1 + p_2)^2}{m_4^2} \quad \text{and} \quad u := \frac{(p_1 + p_4)^2}{m_4^2} \quad (3.10)$$

and extract the dependence on m_4^2 by power counting such that

$$\Phi \left(\begin{array}{c} \overrightarrow{p_2} \text{---} \bullet \text{---} \overrightarrow{p_3} \\ | \quad | \\ \bullet \text{---} \overrightarrow{p_1} \text{---} \bullet \text{---} \overrightarrow{p_4} \end{array} \right) = \frac{\Gamma(2 + \varepsilon) \cdot m_4^{-4-2\varepsilon}}{mp - su - s - mu} \cdot \sum_{n=-1}^{\infty} f_n(s, u, p, m) \varepsilon^n. \quad (3.11)$$

The final set of polynomials in the reduction (after integrating α_1, α_2 and α_4) is

$$S_{\{1,2,4\}} = \left\{ s - p, s + m, s - mp, s + u - p, s + m - p - 1, s(1 + u) + m(u - p), \right. \\ \left. u - p, u + 1, u + 1 - m, p + 1, 1 - m \right\} \quad (3.12)$$

and confines the symbol of the polylogarithms f_n to arbitrary order $n \geq -1$ as explained in section 5.1. In terms of the hyperlogarithms $S_w := L_w(s)$, $U_w := L_w(u)$, $P_w := L_w(p)$ and $M_w := L_w(m)$ we obtain

$$f_{-1} = U_{-1} + S_{-m} - P_{-1} = \ln \frac{(u + 1)(s + m)}{m(p + 1)}, \quad (3.13)$$

$$f_0 = 2S_{0,-m} - 2S_{\frac{m(-u+p)}{u+1}, -m} - U_{-1} - S_{-m}M_0 - 2S_{-m,-m} + 2S_{\frac{m(-u+p)}{u+1}}P_{-1} \\ - 2U_{-1,-1} - S_{p+1-m}P_{-1} + P_{-1} + U_{0,-1} + U_{-1+m,-1} + P_{-1+m}M_0 - P_{0,-1} \\ + S_{mp,-m} - U_{-1+m}M_0 - 2S_{\frac{m(-u+p)}{u+1}}U_{-1} + S_{p+1-m}M_0 - P_{-1+m,-1} - S_{-m} \\ + 2P_{-1,-1} - S_{mp}P_{-1} + S_{p+1-m,-m} \quad (3.14)$$

while f_1, f_2, f_3 and f_4 are supplied in the attached file. Note that f_{-1} and f_0 are given in (4.39) of [31] which serve a successful check of our method. We also computed the special

case $p_1^2 = -m_4^2$ and the setup $p_1^2 = p_2^2 = m_4^2 = 0$ (both introduce a further divergence and thus start proportional to ε^{-2}) to check (4.28) and (4.36) therein.

The possibility to expand all these integrals to arbitrary order in ε (further allowing for shifts $a_e = 1 + \nu_e \varepsilon$ of propagator powers) is to our knowledge new⁷.

3.4.3 Double-triangle with two legs off-shell (four scales)

Consider the second graph of figure 10 with massless propagators and two off-shell momenta $q := p_3^2$, $p := \frac{p_1^2}{q}$ and set $s = \frac{(p_1+p_2)^2}{q}$ and $u = \frac{(p_1+p_4)^2}{q}$. It is linearly reducible along the sequence 3, 4, 5, 2, 1 of edges with final polynomials

$$S_{\{3,4,5,2\}} = \{p - s, 1 - s, 1 - u, p - u, p - us, 1 + p - s - u\} \quad (3.15)$$

which determine the alphabet of the symbol of the functions f_n in the expansion

$$\Phi \left(\begin{array}{ccc} p_2 \rightarrow & 2 & \rightarrow p_3 \\ | & \diagup & | \\ 1 & 5 & 3 \\ | & \diagdown & | \\ p_1 \rightarrow & 4 & \leftarrow p_4 \end{array} \right) = \frac{\Gamma(1+2\varepsilon)q^{-1-2\varepsilon}}{1+p-s-u} \sum_{n=-2}^{\infty} f_n(s, u, p) \varepsilon^n. \quad (3.16)$$

Explicitly, in terms of the hyperlogarithms $S_w := L_w(s)$, $U_w := L_w(u)$ and $P_w := L_w(p)$

$$f_{-2} = \frac{\pi^2}{2} - S_{1,0} + S_{\underline{u},0} - S_{p,0} + S_{\underline{u}}U_0 - U_{p,0} - U_{1,0} + P_0 (S_p + U_p - S_{\underline{u}}) + P_{0,0}, \quad (3.17)$$

$$\begin{aligned} f_{-1} = & 2\zeta_3 + \pi^2 \left(S_{1-u+p} - S_{\underline{u}} - P_0 + U_{1+p} + P_{-1} \right) - 2S_{\underline{u}}U_pP_0 + 2S_{1-u+p}U_pP_0 \\ & + 2U_{1,0,0} - 4P_{0,0,0} + 2P_{-1,0,0} + 2U_{p,0,0} - 2U_{1+p,1,0} - 2S_{1-u+p,1,0} - 2S_{1-u+p,p,0} \\ & + 2S_{\underline{u},1,0} + 2S_{1,0,0} + 2S_{p,0,0} - 2U_{1+p,p,0} - 2S_{\underline{u},0,0} + 2S_{1-u+p,\underline{u},0} + 2S_{\underline{u},p,0} \\ & - 2S_{\underline{u},\underline{u},0} + 2S_{1-u+p,p}P_0 - 2S_{1-u+p,\underline{u}}P_0 + 2S_{1-u+p,\underline{u}}U_0 + 2S_{1-u+p}P_{0,0} \\ & - 2S_pP_{0,0} - 2S_{1-u+p}U_{p,0} + 2S_{\underline{u}}U_{p,0} - 2U_pP_{0,0} + 2U_{1+p}P_{0,0} + 2U_{1+p,p}P_0 \\ & + 2S_{\underline{u}}U_{1,0} - 2S_{1-u+p}U_{1,0} - 2S_{\underline{u},p}P_0 - 2S_{\underline{u},\underline{u}}U_0 + 2S_{\underline{u},\underline{u}}P_0 - 2S_{\underline{u}}U_{0,0} \end{aligned} \quad (3.18)$$

and we supply f_0, f_1 and f_2 in the attached file. Since $\varphi = q\alpha_5 (p\alpha_1\alpha_4 + \alpha_2\alpha_3 + s\alpha_2\alpha_4 + u\alpha_1\alpha_3)$ factorizes, we can in fact perform three integrations of (3.16) in terms of Γ -functions and therefore obtain the two-dimensional integral representation

$$\begin{aligned} \Phi \left(\begin{array}{ccc} p_2 \rightarrow & 2 & \rightarrow p_3 \\ | & \diagup & | \\ 1 & 5 & 3 \\ | & \diagdown & | \\ p_1 \rightarrow & 4 & \leftarrow p_4 \end{array} \right) = & \frac{\Gamma(\text{sdd})\Gamma(D/2 - a_5)\Gamma(D/2 - a_{12})\Gamma(D/2 - a_{34})}{\Gamma(D/2 - \text{sdd})\Gamma(a_1)\Gamma(a_2)\Gamma(a_3)\Gamma(a_4)\Gamma(a_5) \cdot q^{\text{sdd}}} \\ & \times \int_0^\infty x^{a_2-1} dx \int_0^\infty y^{a_4-1} dy \frac{(1+x)^{\text{sdd}-a_{12}}(1+y)^{\text{sdd}-a_{34}}}{(u+x+py+axy)^{\text{sdd}}} \end{aligned} \quad (3.19)$$

which can be immediately expanded in ε (linear reducibility is now obvious). We used this second representation to check the results obtained with the (more demanding) five-dimensional integration (3.16) and also checked the special case $p = 1$ ($p_1^2 = p_3^2$) obtained for f_{-2} and f_{-1} in [29] as $\mathcal{I}_{182}^{(B)}$.

⁷General results in terms of hypergeometric functions are given in [32], however it is not clear how to expand these to arbitrary orders.

3.4.4 Double-triangle with two legs off-shell and two masses (six scales)

We now consider the same two-loop graph, but introduce two non-zero masses at the edges 3 and 4. This removes a sub divergence such that the expansion

$$\Phi \left(\begin{array}{c} p_2 \rightarrow \bullet \xrightarrow{2} \bullet \xrightarrow{5} \bullet \xrightarrow{3} p_3 \\ \bullet \xrightarrow{1} \bullet \xrightarrow{4} \bullet \xrightarrow{3} p_4 \\ p_1 \rightarrow \bullet \end{array} \right) = \frac{\Gamma(1+2\varepsilon)}{(p+q-s-u)m_3^{2+4\varepsilon}} \sum_{n=-1}^{\infty} f_n(p, s, u, q, m) \cdot \varepsilon^n \quad (3.20)$$

begins with ε^{-1} . In terms of the dimensionless variables

$$s := \frac{(p_1 + p_2)^2}{m_3^2} \quad u := \frac{(p_1 + p_4)^2}{m_3^2} \quad p := \frac{p_1^2}{m_3^2} \quad q := \frac{p_3^2}{m_3^2} \quad m := \frac{m_4^2}{m_3^2}, \quad (3.21)$$

the symbols of all f_n take letters in $\{s, u, p, q, m\} \cup S_{\{3,4,5,2\}}$ for the final polynomials

$$S_{\{3,4,5,2\}} = \left\{ 1 - m, p + m, p - s, p - u, 1 + q, q - s, s + m, q - u, 1 + u, pq - us, s - qm, \right. \\ \left. p - um, 1 - p - m + u, p - s - u + q, p - s + qm - um, 1 - s - m + q, \right. \\ \left. s - pq - qm + us, p - us - um + pq, pq + p - us - s + qm - um \right\}. \quad (3.22)$$

Abbreviating $S_w := L_w(s)$, $U_w := L_w(u)$, $M_w := L_w(m)$, $P_w := L_w(p)$ and $Q_w := L_w(q)$ as before, the leading term becomes

$$f_{-1} = M_0 (Q_{0,-1+m} - P_u U_{-1+m} + S_q Q_{-1+m} - U_{0,-1+m}) - S_{m(-u+q),qm,-m} + P_{\frac{us}{q},s} S_{-m} \\ - S_{-m} P_{s+um-qm,s} + P_u U_{-1+m,-1} - S_q Q_{-1+m,-1} + P_{u,-m+u+1} (U_{-1} - M_0) \\ + U_{-1} \left(P_{\frac{us}{q},um} - P_{s+um-qm,um} - P_{u,um} \right) + Q_{-1} \left(S_{m(-u+q),qm} - S_{0,qm} + S_{q,qm} \right) \\ + P_{s+um-qm,s,-m} - P_{\frac{us}{q},um,-m} + S_{0,0,-m} - P_{\frac{us}{q},s,-m} + P_{\frac{us}{q},0,-m} - S_{0,\frac{m(-u+q)}{u+1},-m} \\ - S_{q,qm,-m} + S_{q,-m+q+1,-m} - P_{u,-m+u+1,-m} + S_{0,qm,-m} + P_{s+um-qm,um,-m} \\ + P_{\frac{us}{q},-\frac{-us-s-um+qm}{q+1},-m} + U_{0,-1+m,-1} + S_{q,0,-m} - P_{u,0,-m} - P_{s,0,-m} - Q_{0,-1+m,-1} \\ - P_{s+um-qm,-\frac{-us-s-um+qm}{q+1},-m} + S_{m(-u+q),\frac{m(-u+q)}{u+1},-m} - S_{m(-u+q),0,-m} + P_{u,um,-m} \\ + (U_{-1} - Q_{-1}) \left(S_{m(-u+q),\frac{m(-u+q)}{u+1}} - S_{0,\frac{m(-u+q)}{u+1}} \right) + S_{m(-u+q)} (-U_{0,-1} + Q_{0,-1}) \\ + (S_{-m} + U_{-1} - Q_{-1}) \left[P_{s+um-qm,-\frac{-us-s-um+qm}{q+1}} - P_{\frac{us}{q},-\frac{-us-s-um+qm}{q+1}} \right] + P_s S_{0,-m} \\ + \left(P_{s+um-qm} - P_{\frac{us}{q}} \right) \left[S_{\frac{m(-u+q)}{u+1}} (U_{-1} - Q_{-1}) - S_{\frac{m(-u+q)}{u+1},-m} + S_{qm} Q_{-1} - S_{qm,-m} \right] \\ + S_{q,-m+q+1} (-Q_{-1} + M_0) + P_{s+um-qm} (Q_{0,-1} - S_{0,-m} - U_{0,-1}) \quad (3.23)$$

while f_0 , f_1 and f_2 are provided in the ancillary file. Their symbols do not involve the letters $\{pq + qm - us - s, us + um - pq - p\}$ and might suggest that these are indeed superfluous and could be removed from (3.22) by an improved reduction algorithm.

A completely independent check of our analytic results is possible by numeric integration as shown in table 2. The number in the last row counts the polylogarithms that occur

	f_{-1}	f_0	f_1	f_2	f_3
[7]	-0.604907	+0.104586	-1.03958	+0.141365	-1.26899
exact	-0.604918601	+0.104721339	-1.039167083	+0.142116843	-1.267745643
terms	66	668	4558	26360	139502

Table 2. Numeric results for (3.20) at $m_3 = 1$, $m = 2$, $u = 0.75$, $q = 0.5$, $s = 0.2$ and $p = 0.1$ from sector decomposition and first digits of our exact analytic result.

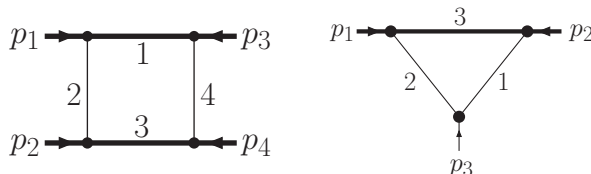


Figure 11. A box with two massive internal lines (1 and 3) that are not adjacent is not linearly reducible. The infrared divergence of the (linearly reducible) triangle graph is studied in example 5.2.

in the basis as used in (3.23). Furthermore we checked that the on-shell equal mass limit ($p, q \rightarrow -1$ and $m \rightarrow 1$) of f_{-1} reproduces the result obtained in [28], equations (3.9) and (3.10a).

4 Extending linear reducibility

We have seen Feynman graphs that are not linearly reducible but still are known to evaluate to polylogarithms. To us this strongly suggests that in these cases, the Schwinger parameters are not optimal and we expect a different parametrization to exist that allows for parametric integration.

This idea was already mentioned in [5] and we like to demonstrate how a rational parametrization of quadrics can indeed restore linear reducibility (in a different set of variables). In principle, this technique can always be applied if the obstruction to linear reducibility is given by a single quadratic polynomial.

4.1 One-loop example: box with two masses vis-à-vis

Consider the on-shell massive box with $p_1^2 = p_2^2 = p_3^2 = p_4^2 = -m^2$ for two massive propagators $m_1 = m_3 = m$ and massless $m_2 = m_4 = 0$ as shown in figure 11. In contrast to the case of section 3.4.2 where the massive propagators are adjacent, this graph is not linearly reducible: With $s = (p_1 + p_2)^2$ and $t = (p_1 + p_3)^2$, its graph polynomials are

$$\psi = \alpha_1 + \alpha_2 + \alpha_3 + \alpha_4 \quad \text{and} \quad \varphi = s\alpha_1\alpha_3 + t\alpha_2\alpha_4 + m^2(\alpha_1 + \alpha_3)^2 \quad (4.1)$$

and φ is only linear in α_2 and α_4 . Reducing (integrating) α_4 we obtain the set

$$S_{\{4\}} = \left\{ \alpha_1 + \alpha_2 + \alpha_3, s\alpha_1\alpha_3 + m^2(\alpha_1 + \alpha_3)^2, R \right\} \quad \text{where the resultant} \quad (4.2)$$

$$R := [\psi, \varphi]_{\alpha_4} = s\alpha_1\alpha_3 + m^2(\alpha_1 + \alpha_3)^2 - t\alpha_2(\alpha_1 + \alpha_3) \quad (4.3)$$

is irreducible and quadratic in all remaining Schwinger parameters, therefore prohibiting any further integration. To proceed we change variables according to

$$\frac{s}{m^2} = \frac{(1-x)^2}{x} \quad \frac{t}{m^2} = \frac{(1-y)^2}{y} \quad \alpha_2 = \widetilde{\alpha}_2(\alpha_1 + x\alpha_3) \quad \alpha_4 = \widetilde{\alpha}_4(x\alpha_1 + \alpha_3). \quad (4.4)$$

On one hand we reparametrized the kinematics via x and y to rationalize roots that would otherwise appear in the result (this is analogous to (3.4)), while afterwards

$$\varphi = \frac{m^2}{x}(\alpha_1 + x\alpha_3)(x\alpha_1 + \alpha_3) + \frac{m^2}{y}(1-y)^2\alpha_2\alpha_4 \quad (4.5)$$

suggests to introduce the variables $\widetilde{\alpha}_2$ and $\widetilde{\alpha}_4$ of (4.4) with the effect that

$$\varphi = \frac{m^2}{xy}(\alpha_1 + x\alpha_3)(x\alpha_1 + \alpha_3) \left[y + x(1-y)^2\widetilde{\alpha}_2\widetilde{\alpha}_4 \right] \quad (4.6)$$

factors linearly in these new parameters. It follows that $\widetilde{R} = [\psi, y + x(1-y)^2\widetilde{\alpha}_2\widetilde{\alpha}_4]_{\widetilde{\alpha}_4}$ is linear in α_1 and α_3 allowing for a further integration. Calculating the reduction shows that we can finally also integrate $\widetilde{\alpha}_2$ and obtain the final set of polynomials

$$S_{\{\widetilde{\alpha}_2, \alpha_3, \widetilde{\alpha}_4\}} = \{x+1, x-1, y+1, y-1, xy+1, x+y\} \quad (4.7)$$

which together with $\{x, y\}$ define the alphabet of the symbol of the resulting function of x and y . This coincides with the observation made in [30] upon a study of its differential equations. With the described change of variables we applied the parametric integration procedure and cross-checked our result successfully with the expansion given as (2.27) in [30].

4.2 Three-loop example: K_4

We return to the complete graph K_4 of figure 4 with massless on-shell kinematics $p_1^2 = \dots = p_4^2 = m_1 = \dots = m_6 = 0$ already mentioned in section 3.1. In this case, after integrating say α_2 we can not proceed further because again the resultant $R := [\psi, \varphi]_2 \in S_{\{2\}}$ is irreducible and quadratic in all Schwinger parameters. But its discriminant⁸

$$D_{\alpha_3}(R) = \alpha_1^2(\alpha_1\alpha_6 + \alpha_6\alpha_4 + \alpha_4\alpha_5 + \alpha_6\alpha_5)^2 \quad (4.8) \\ \times \left[\alpha_6^2 t^2 \alpha_4^2 - 2t\alpha_4\alpha_6(-t\alpha_6 + s\alpha_4 - s\alpha_6)\alpha_5 + (s\alpha_6 + s\alpha_4 + t\alpha_6)^2 \alpha_5^2 \right]$$

becomes a perfect square if we introduce a new variable ξ and reparametrize

$$\alpha_5 = \frac{t\alpha_4\alpha_6(s\alpha_6 + t\alpha_6 + \xi)}{\xi(s\alpha_6 + s\alpha_4 + t\alpha_6 + \xi)}. \quad (4.9)$$

Hence after this transformation, R factorizes linearly in α_3 and indeed the polynomial reduction shows that we obtain linear reducibility along the sequence $\alpha_2, \alpha_3, \alpha_1, \alpha_4, \xi$ ($\alpha_6 = 1$) of integrations. The final set is $\{s+t\}$ and proves that to all orders, $\Phi(K_4) s^{3\varepsilon}$ is a harmonic polylogarithm of $\frac{t}{s}$ which was observed before in [18]. We performed the explicit integrations and reproduced the result up to order ε^2 (polylogarithms of weight six) given in (B.1) of [18].

⁸For $R = A\alpha_3^2 + B\alpha_3 + C$ the discriminant with respect to α_3 is $D_{\alpha_3}(R) = B^2 - 4AC$.

5 Divergences in Schwinger parameters

The method of parametric integration relies on convergent integral representations of the quantities (functions) to be computed, but many Feynman integrals are divergent. While ultraviolet divergences can be renormalized on the level of the integrand directly⁹ and then result in a convergent parametric integral representation (see for example [34]), the cancellation of infrared divergences is more subtle. In practical calculations it turned out to be most useful to assign values also to infinite integrals in terms of a regularization prescription, therefore separating the two problems of calculation of the integrals and renormalization of their divergences.

In this section we briefly explain why the most widely employed *dimensional regularization*¹⁰ is perfectly adapted to parametric integration and explain a general method to generate convergent integral representations of dimensionally regulated, divergent Feynman integrals. Note that usually this task is solved by the method of *sector decomposition* [35, 36] which is publicly available as [7, 21, 37]. But this approach introduces various changes of variables and decomposes the original integrand into many summands, which would need to be analyzed separately for linear reducibility. Furthermore finite integrals are obtained by subtraction of counterterms, and we argued in [10] that it is in general unclear how this effects the polynomial reduction.

Therefore we prefer an expression in the original Schwinger parameters, involving only the polynomials ψ and φ in denominators. The criteria of convergence here are well-known and we merely employ integration by parts, so we do certainly not assume our result to be new but rather a reformulation. Nevertheless it is crucial for our study of linear reducibility.

We investigate a projective parametric integral $[\prod_e \int_0^\infty d\alpha_e] F\delta(H)$ which we denote by $\int F\Omega$ (so Ω is the canonical volume form on $\mathbb{RP}^{|E|-1}$). The parametric integrand is a rational function of the α_e and contains exponents that can depend on D and the propagator powers a_e . Given disjoint sets $J, K \subset E$ of edges,

$$F_J^K := F|_{\alpha_e \mapsto \lambda\alpha_e \ \forall e \in J \text{ and } \alpha_e \mapsto \lambda^{-1}\alpha_e \ \forall e \in K} \in \mathcal{O}\left(\lambda^{\deg_J^K(F)}\right) \quad \text{at } \lambda \rightarrow 0 \quad (5.1)$$

defines a degree $\deg_J^K(F)$ of vanishing¹¹ of F when all α_e with $e \in J$ tend to zero and $\alpha_e \rightarrow \infty$ for $e \in K$. Denoting the associated degree of divergence by

$$\omega_J^K(F) := |J| - |K| + \deg_J^K(F), \quad (5.2)$$

we recall the well-known finiteness result

Lemma 5.1. *Let all non-zero coefficients of φ be positive¹² and $\omega_J^K > 0$ for all disjoint $J, K \subset E$ with $\emptyset \neq J \dot{\cup} K \subsetneq E$. Then $\int F\Omega$ is absolutely convergent.*

⁹Most standard text books on quantum field theory explain the BPHZ method, e.g. [3, 33].

¹⁰A definition of this scheme in terms of convergent *momentum space* integrals is given in [33].

¹¹So $\deg_J^K(F)$ is the unique number s such that $\lim_{\lambda \rightarrow 0} [\lambda^{-s} \cdot F_J^K]$ exists and is non-zero.

¹²Otherwise divergences can occur inside the integration domain. Some examples of this more complicated situation are explained in [38].

Proof. The positivity condition implies that F is continuous on the interior $(0, \infty)^{|E|}$, hence F can only have singularities on the boundary $\bigcup_e (B_e^0 \cup B_e^\infty)$ where $B_e^\bullet := \{\alpha_e = \bullet\}$. Cover the domains $\mathbb{R}_+ = (0, 1] \cup [1, \infty)$ and transform $\alpha_e \rightarrow \alpha_e^{-1}$ on $(0, 1]$ such that

$$\int F\Omega = \sum_{I \subseteq E} \left[\prod_{e \notin I} \int_1^\infty d\alpha_e \right] \left[\prod_{e \in I} \int_1^\infty \frac{d\tilde{\alpha}_e}{\tilde{\alpha}_e^2} \right] F|_{\alpha_e = \tilde{\alpha}_e^{-1} \ \forall e \in I}.$$

Now $\omega_J^K > 0$ for all $K \subset E \setminus I$ and $J \subset I$ translates into the convergence condition¹³ of Weinberg's Theorem [39]. \square

This result is well-known and a graph-theoretic interpretation of ω_J^K is possible, see for example the appendix E.1 of [2] and references therein.

Example 5.2. *The triangle graph G of figure 11 with one internal mass $m = m_3$ and light-like $p_3^2 = 0$ is linearly reducible with the graph polynomials*

$$\psi = \alpha_1 + \alpha_2 + \alpha_3 \quad \text{and} \quad \varphi = \alpha_3 \left(m^2 \psi + p_1^2 \alpha_2 + p_2^2 \alpha_1 \right). \quad (5.3)$$

For $D = 4 - 2\varepsilon$ and $a_1 = a_2 = a_3 = 1$, the parametric integral representation

$$\Phi(G) = \int \frac{d^D k}{\pi^{D/2}} \frac{1}{(k^2 + m^2)(k + p_2)^2(k - p_1)^2} = \Gamma(1 + \varepsilon) \int \frac{\Omega}{\psi^{1-2\varepsilon} \varphi^{1+\varepsilon}}$$

diverges at $\varepsilon = 0$: $\omega_{\{3\}}^\emptyset = \omega_\emptyset^{\{1,2\}} = -\varepsilon$ represent a logarithmic divergence. It is apparent from the factor $\alpha_3^{-1-\varepsilon}$ in the integrand.

5.1 Analytic regularization

For a choice of disjoint $J, K \subset E$ we can regard λ as a new integration variable by inserting the factor $1 = \int_0^\infty d\lambda \delta(\lambda - \alpha_J - \alpha_K^{-1})$ where $\alpha_J := \sum_{e \in J} \alpha_e$. After rescaling α_e by λ (λ^{-1}) for $e \in J$ ($e \in K$), we see

$$\int F\Omega = \int \Omega \delta(1 - \alpha_J - \alpha_K^{-1}) \int_0^\infty \frac{d\lambda}{\lambda} \lambda^{\omega_J^K} \cdot \widetilde{F}_J^K(\lambda)$$

where $\widetilde{F}_J^K := F_J^K \cdot \lambda^{-\deg_J^K}$ is finite at $\lambda \rightarrow 0$. The partial integration

$$\int_0^\infty \frac{d\lambda}{\lambda} \lambda^{\omega_J^K} \cdot \widetilde{F}_J^K(\lambda) = \frac{\lambda^{\omega_J^K}}{\omega_J^K} \widetilde{F}_J^K(\lambda) \Big|_{\lambda=0}^\infty - \frac{1}{\omega_J^K} \int_0^\infty d\lambda \cdot \lambda^{\omega_J^K} \frac{\partial}{\partial \lambda} \widetilde{F}_J^K(\lambda) \quad (5.4)$$

has vanishing boundary contribution when $\omega_J^K > 0$ and $F_J^K(\lambda)$ falls off at $\lambda \rightarrow \infty$ faster than $\lambda^{|J|-|K|}$, so in particular whenever $\int F\Omega$ is convergent.

The analytically regularized functions associated to both integrals in (5.4) are therefore equal, because they are meromorphic in the analytic regulators $\{D\} \cup \{a_e: e \in E\}$ and coincide in the domain of absolute convergence of $\int F\Omega$ (which is non-empty as proven already in [40]).

¹³As the projective integral is only $(E-1)$ dimensional, we can drop constraints on ω_J^K when $J \cup K = E$.

Changing back to the original variables, we conclude that $\int \Omega F = \int \Omega \mathcal{D}_J^K(F)$ where

$$\mathcal{D}_J^K := 1 - \frac{1}{\omega_J^K} \left[\sum_{e \in J} \partial_e \alpha_e - \sum_{e \in K} \partial_e \alpha_e \right] = \frac{1}{\omega_J^K} \left[\deg_J^K - \sum_{e \in J} \alpha_e \partial_e + \sum_{e \in K} \alpha_e \partial_e \right] \quad (5.5)$$

denotes a differential operator with $\partial_e := \frac{\partial}{\partial \alpha_e}$.

Example 5.3 (Triangle graph of figure 11). *With respect to $J = \{3\}$ and $K = \emptyset$ we have $\widetilde{F}^K = \psi^{2\varepsilon-1} \cdot [m^2\psi + p_2^2\alpha_1 + p_1^2\alpha_2]^{-1-\varepsilon}$ with $\omega_J^K = -\varepsilon$ and deduce*

$$\int \frac{\Omega}{\psi^{1-2\varepsilon}\varphi^{1+\varepsilon}} = \frac{1}{\varepsilon} \cdot \int \frac{\Omega}{\alpha_3^\varepsilon} \frac{\partial}{\partial \alpha_3} \widetilde{F} = \frac{1}{\varepsilon} \cdot \int \frac{\Omega \alpha_3}{\psi^{1-2\varepsilon}\varphi^{1+\varepsilon}} \left[\frac{2\varepsilon-1}{\psi} - \frac{(1+\varepsilon)\alpha_3 m^2}{\varphi} \right] \quad (5.6)$$

as an identity between analytically regularized integrals. In their joint domain $\varepsilon < 0$ of convergence, the boundary term $\left. \frac{\alpha_3^{-\varepsilon} \widetilde{F}}{-\varepsilon} \right|_{\alpha_3=0}^\infty$ is well-defined and vanishes. Note that the integral on the right-hand-side of (5.6) has an increased regime $\varepsilon < 1$ of convergence.

We can summarize our results in the form of

Lemma 5.4. *For any disjoint subsets $J, K \subset E$ with $\emptyset \neq J \cup K \subsetneq E$, the new parametric integrand $\widetilde{F} := \mathcal{D}_J^K(F)$ fulfils*

1. $\int F \Omega = \int \widetilde{F} \Omega$ as analytically regularized integrals,
2. $\omega_{J'}^{K'}(\widetilde{F}) \geq \omega_{J'}^{K'}(F)$ for any disjoint $J', K' \subset E$ and
3. $\omega_J^K(\widetilde{F}) \geq 1 + \omega_J^K(F)$ increases at least by one.

Properties 2 and 3 are probably most evident by introducing simultaneously variables λ_J^K for all disjoint J, K and rescaling $\alpha_e \mapsto \alpha_e \prod_{e \in J, J \cap K = \emptyset} \lambda_J^K \prod_{e \in K, J \cap K = \emptyset} (\lambda_J^K)^{-1}$ such that

$$F = \prod_{J \cap K = \emptyset} (\lambda_J^K)^{\deg_J^K} \cdot R \quad \text{where} \quad R = \prod_{p \in \mathcal{P}} p^{a_p} \quad (5.7)$$

factors into irreducible polynomials¹⁴ $p \in \mathcal{P}$ (with exponents a_p) in Schwinger parameters α_e , the scaling variables λ_J^K and kinematic invariants. Now the action of \mathcal{D}_J^K on F equals replacing R by $\lambda_J^K \partial_{\lambda_J^K} R$ (and dividing by $-\omega_J^K$), but

$$\partial_{\lambda_J^K} R = R \sum_{p \in \mathcal{P}} \frac{a_p}{p} \cdot \partial_{\lambda_J^K}(p)$$

can only factor in the numerator (then possibly contributing additional powers of some $\lambda_{J'}^{K'}$), while the extra denominators p do by construction not introduce new divergences (which would correspond to poles at $\lambda_{J'}^{K'} \rightarrow 0$).

Corollary 5.5. *Finitely many applications of operators \mathcal{D}_J^K on F suffice to generate a representation of $\int F \Omega = \int \widetilde{F} \Omega$ with a convergent parametric integrand \widetilde{F} (all $\omega_J^K(\widetilde{F})$ are positive).*

¹⁴For scalar Feynman integrals we have only the irreducible factors of ψ and φ in \mathcal{P} .

For example, when $\int F\Omega$ is regulated by D alone¹⁵, we identify divergences $\omega_J^K|_{\varepsilon=0} \geq 0$ by power-counting and apply \mathcal{D}_J^K sufficiently often until $\omega_J^K|_{\varepsilon=0} > 0$.

Crucially, the representation \tilde{F} obtained this way can only contain ψ and φ with non-integer or negative exponents. Therefore, any term in its ε -expansion lies in

$$\mathbb{Q} \left[\Theta \cup \{\alpha_e : e \in E\} \cup \{\psi^{-1}, \varphi^{-1}\} \cup \{\ln \psi, \ln \varphi\} \right] \quad (5.8)$$

and can be integrated using hyperlogarithms precisely when the graph under consideration is linearly reducible. Put differently, the partial integrations \mathcal{D}_J^K do not affect the polynomial reduction.

We applied this technique for all explicit computations of subdivergent integrals in this article, namely example 3.2, $\Delta_{3,14}$ from example 3.5 and all results of section 3.4.

6 Summary and outlook

We extended the method of parametric integration to divergent, analytically regularized Feynman integrals G for linearly reducible G that may depend on multiple kinematic invariants. Several non-trivial examples were shown and explicit new results given in terms of polylogarithms. Let us stress that such a graph G can in principle be computed

- to arbitrary order in ε , expanded near any even dimension $D|_{\varepsilon=0} \in 2\mathbb{N}$,
- including any tensor structure (loop momenta in the numerator); in particular the form-factor-decomposition is automatic in the parametric representation and we do not need a reduction to master integrals in the integration-by-parts (IBP) sense,
- with arbitrary powers $a_e = n_e + \varepsilon\nu_e$ of propagators for $n_e \in \mathbb{Z}$.

Practically however, tensor structure and sub divergences (via the integrand preparation of section 5) can result in very complicated initial integrands, involving high powers of ψ and/or φ in the denominator and a huge polynomial in the numerator. Such cases require a simplification before the computation and it seems possible to apply the idea of integration by parts directly to these parametric integrands which we will try to return to in the future.

In this context also note that the procedure suggested by lemma 5.4 seems to generate unnecessarily complicated integrands in the case of overlapping divergences.

Example 6.1. *In the case of the two-loop graph of section 3.4.3, the original parametric integrand has many divergences. E.g. we find $\omega_\emptyset^{\{\alpha_1, \alpha_2, \alpha_3, \alpha_4\}} = -2\varepsilon$, $\omega_\emptyset^{\{\alpha_3, \alpha_4, \alpha_5\}} = -\varepsilon$ and $\omega_\emptyset^{\alpha_3, \alpha_4} = -\varepsilon$, and integrating these partially yields the convergent integrand*

$$\frac{(3\varepsilon - 2)(3\varepsilon - 1)}{2\varepsilon^3} \frac{\alpha_5^2(\alpha_3 + \alpha_4)(\alpha_1 + \alpha_2)}{\varphi^{1+2\varepsilon}\psi^{4-3\varepsilon}} [2(\alpha_1 + \alpha_2)(\alpha_3 + \alpha_4) + (3\varepsilon - 1)\alpha_5(\alpha_1 + \alpha_2 + \alpha_3 + \alpha_4)]$$

which we used in the computations of (3.17) and (3.18). But note that (3.16) has only a pole in ε of second order and indeed we find that the term $\propto \varepsilon^{-3}$ integrates to zero. In

¹⁵This is not always possible; in general divergences require the exponents a_e as analytic regulators.

contrast, the much better adapted representation (3.19) has a manifest second order pole in ε and no divergences in the parametric integral. It is considerably more efficient to evaluate.

Therefore one might try to find more economic ways of generating analytically regularized, convergent integrands (with only φ and ψ raised to non-integer or negative powers). Note however that an integration-by-parts reduction of the parametric integrands as suggested above could also partially solve this problem.

Apart from these technicalities, conceptually we face the important open question to combinatorially characterize the linearly reducible graphs in the presence of non-trivial dependence on kinematic invariants. As we recalled in section 2, only in the massless propagator case such a result is available in form of theorem 2.1. It exploits that $\varphi_G = \psi_{G_\bullet}$ where G_\bullet denotes G after identifying the two vertices attached to the external momenta and follows from the plethora of identities and factorization formulas among these ψ - and the related *Dodgson*-polynomials [9, 41]. But still this covers only a subset of the linearly reducible topologies and we had to explicitly examine the graph polynomials (using a polynomial reduction algorithm) to arrive at theorem 2.2.

Hence regarding non-trivial kinematics, it will be inevitable to incorporate the new polynomial φ and to find analogous factorization properties in order to arrive at combinatorial criteria sufficient for linear reducibility. We hope that the plentiful positive examples in this article motivate progress in this direction.

Even further, the examples of section 4 suggest that in some cases we must abandon the original Schwinger parameters and should look for other representations. A systematic study of suitable changes of variables and in particular criteria exhibiting when these can regain linear reducibility is certainly a demanding but worthwhile project.

A Polynomial reduction and linear reducibility

In a parametric representation, we are naturally working with polylogarithmic functions of several variables: To begin with, from expanding (1.1) in say ε we obtain integrands

$$F \in \mathbb{Q}[\psi^{-1}, \varphi^{-1}, \log \psi, \log \varphi, \{\alpha_e, \alpha_e^{-1}, \log \alpha_e : e \in E\}, \Theta].$$

Hence these are iterated integrals in the Schwinger- and kinematic variables and we call

$$\mathcal{B}(S) := \left\{ \sum_i \frac{f_i}{g_i} \int d \log(h_{i,1}) \cdots \int d \log(h_{i,j}) : g_i, h_{i,j} \in S \cup \{\alpha_e : e \in E\} \cup \Theta \right\} \quad (\text{A.1})$$

(with rational f_i) the functions *with symbol in*¹⁶ S , according to the *symbol calculus* of [42, 43] and also following [8]. So in particular $F \in \mathcal{B}(S_\theta)$ for $S_\theta := \{\psi, \varphi\}$. In this language, the essence of the polynomial reduction algorithm of [5] can be stated as

¹⁶We always allow for $d \log \alpha_e$ and $d \log s$ of kinematic invariants $s \in \Theta$ and do not write these in S .

Lemma A.1. *If $h \in \mathcal{B}(S)$ and all $f \in S$ are linear $f = A_f \alpha_e + B_f$ in α_e and $H = \int_0^\infty h \, d\alpha_e$ converges, then $H \in \mathcal{B}(S_e)$ where S_e is the set of irreducible factors¹⁷ of*

$$\{A_f, B_f: f \in S\} \text{ and the resultants } \{[f, g]_{\alpha_e} := A_f B_g - A_g B_f: f, g \in S\}. \quad (\text{A.2})$$

Example A.2. *From the parametric integrand F of (3.19) we read off the polynomials $S_\emptyset = \{u + x + py + sxy, 1 + x, 1 + y\}$ such that $F \in \mathcal{B}(S_\emptyset)$. Using (A.2) we first deduce $\int_0^\infty F \, dy \in \mathcal{B}(S_y)$ with $S_y = \{1 + x, u + x, p + sx, u + x - p - sx\}$ and then apply (A.2) again to obtain $\int \int_0^\infty F \, dy \, dx \in \mathcal{B}(S_{y,x})$. In fact we reproduce (3.15) since*

$$S_{y,x} := (S_x)_y = \{u - p, 1 - s, 1 - u, p - s, u - 1 - p + s, p - su\}.$$

Under the assumptions of this lemma, [5] describes an entirely combinatorial-algebraic algorithm to effectively compute the integral $\int_0^\infty h \, d\alpha_e$. Let us stress that in particular it does not need any numeric evaluations or separate input of boundary values to fix integration constants, which sometimes is a problem for example within the method of differential equations. Details of our implementation will be given in the forthcoming publication of our program.

We therefore formulate the prerequisite for parametric integration as

Definition A.3. *G is called linearly reducible if for some ordering e_1, \dots, e_N of its edges there exist sets $S_n \subset \mathbb{Q}[\alpha_{n+1}, \dots, \alpha_N]$ of polynomials for all $0 \leq n < N$ ($S_0 := S_\emptyset$) such that for any convergent parametric integrand $F \in \mathcal{B}(S_\emptyset)$ the partial integrals*

$$f_n := \left[\prod_{e=1}^n \int_0^\infty d\alpha_e \right] F \text{ lie in } \mathcal{B}(S_n) \text{ for any } n + 1 < N = |E| \quad (\text{A.3})$$

and all $g \in S_n$ are linear in α_{n+1} .

As in example A.2, repeated application of lemma A.1 can suffice to prove linear reducibility in simple cases (c.f. the *Fubini* algorithm in [5]), but for this article we employed the way more powerful method of *compatibility graphs* that was developed in [9]. This algorithm computes for each set $I \subset E$ of edges a set $S_I \subset \mathbb{Q}[\{\alpha_e: e \notin I\}]$ of irreducible polynomials such that the partial integrals $f_I := \prod_{e \in I} \int_0^\infty d\alpha_e F$ are analytic outside the *Landau variety* $L_I = \bigcup_{g \in S_I} \{g = 0\}$ defined in [9]. These sets S_I are typically much smaller than the upper bounds obtained by lemma A.1 alone.

A.1 Hyperlogarithms

The direct integration of iterated integrals of many variables is possible symbolically as shown in [8], whereas our approach of [5] is to consider the dependence of the integrand on the next integration variable $z = \alpha_n$ only, which reduces the function to the one-dimensional integrals of

¹⁷Here we drop pure constants c (since $d \log c = 0$) and monomials.

Definition A.4. For any word $w \in \Sigma^\times$ in letters $\{\omega_\sigma : \sigma \in \Sigma\}$ over a finite set $0 \in \Sigma \subset \mathbb{C}$, the associated hyperlogarithm [44] is the iterated integral defined by

$$L_{\omega_0^n}(z) := \frac{\log^n z}{n!} \quad \text{for any } n \in \mathbb{N}_0 \quad \text{and} \quad L_{\omega_\sigma w}(z) := \int_0^z \frac{dz'}{z' - \sigma} L_w(z'). \quad (\text{A.4})$$

Remark A.5. These functions are analytic and in general multi-valued on $\mathbb{C} \setminus \Sigma$, but uniquely defined upon restriction to $z \in \mathbb{C} \setminus (-\infty, 0]$ and $|z| < \min_{0 \neq \sigma \in \Sigma} |\sigma|$. Also called Goncharov polylogarithms, we write

$$G(\sigma_1, \dots, \sigma_n; z) := L_{\sigma_1 \dots \sigma_n}(z) := L_{\omega_{\sigma_1} \dots \omega_{\sigma_n}}(z) \quad (\text{A.5})$$

and can identify them with a special family of multiple polylogarithms: For arbitrary $\sigma_1, \dots, \sigma_r \in \Sigma \setminus \{0\}$, $n_1, \dots, n_r \in \mathbb{N}$ and $|z| < \min_{1 \leq j \leq r} |\sigma_j|$,

$$L_{\omega_0^{n_r-1} \omega_{\sigma_r} \dots \omega_0^{n_2-1} \omega_{\sigma_2} \omega_0^{n_1-1} \omega_{\sigma_1}}(z) = (-1)^r \text{Li}_{n_1, \dots, n_r} \left(\frac{\sigma_2}{\sigma_1}, \dots, \frac{\sigma_r}{\sigma_{r-1}}, \frac{z}{\sigma_r} \right). \quad (\text{A.6})$$

This construction and partial fractioning make it obvious that any function

$$f \in L(\Sigma) := \mathbb{Q} \left[z, \left\{ \frac{1}{z - \sigma} : \sigma \in \Sigma \right\}, \{L_w : w \in \Sigma^\times\} \right] \quad (\text{A.7})$$

in the algebra $L(\Sigma)$ spanned by the hyperlogarithms has a primitive $\partial_z F(z) = f(z)$,

$$F \in \mathbb{Q} \left[\Sigma \cup \left\{ \frac{1}{\sigma_i - \sigma_j} : \sigma_i \neq \sigma_j \text{ from } \Sigma \right\} \right] \otimes L(\Sigma)$$

possibly involving the additional denominators $\sigma_i - \sigma_j$. This mirrors lemma A.1 since

$$f_I \in L(\Sigma_{I,e})(\alpha_e) \quad \text{with} \quad \Sigma_{I,e} := \{0\} \cup \bigcup_{f \in S_I} \{\text{zeros of } f \text{ with respect to } \alpha_e\} \quad (\text{A.8})$$

whenever $f_I \in \mathcal{B}(S_I)$. The final answer $f = f|_{E|-1}$ after integrating out all Schwinger variables (but $\alpha_{|E|} = 1$) has a symbol in $f \in \mathcal{B}(S_{|E|})$.

To represent a function $f \in \mathcal{B}(S)$ in terms of one-dimensional iterated integrals we choose an order s_1, \dots, s_n of the remaining variables Θ and express f in the form¹⁸

$$f \in L(\Sigma_{s_1})(s_1) \otimes \dots \otimes L(\Sigma_{s_n})(s_n) \quad (\text{A.9})$$

where $\Sigma_{s_i} = \{0\} \cup \{\text{zeros of } S^{(i)} \text{ w.r.t. } s_i\}$ and we set $S^{(1)} := S$ and recursively define $S^{(i+1)}$ as the irreducible factors¹⁹ of $\lim_{s_i \rightarrow 0} S^{(i)}$.

Example A.6. If we chose the order $0 < s \ll u \ll p$ of variables, we can write the integrals f of the expansion coefficients F of the integrand (3.19) in the form

$$f \in L \left(\left\{ 0, 1, p, 1 + p - u, \frac{p}{u} \right\} \right) (s) \otimes L(\{0, 1, p, 1 + p\})(u) \otimes L(\{0, -1\})(p) \quad (\text{A.10})$$

¹⁸This corresponds to fixing the path of integration in the iterated integral to the piecewise linear $(0, \dots, 0) \rightarrow (0, \dots, 0, s_n) \rightarrow (0, \dots, 0, s_{n-1}, s_n) \rightarrow \dots \rightarrow (0, s_2, \dots, s_n) \rightarrow (s_1, \dots, s_n)$. The discussion in section 2.7 of [30] might further clarify this process.

¹⁹Again we omit constants and monomials as these are explicitly taken care of by $0 \in \Sigma_{s_i}$.

by taking $S^{(1)}$ from (3.15) and deducing $S^{(2)} = \lim_{s \rightarrow 0} S^{(1)} = \{u - p, 1 - u, u - 1 - p\}$ and $S^{(3)} = \lim_{u \rightarrow 0} S^{(2)} = \{1 + p\}$. Indeed we find precisely the letters given in (A.10) in our results like (3.17), (3.18).

Example A.7. The final set $S_{|E|} = \Sigma_{\Delta} \cup \{z\bar{z} - 1\}$ in the polynomial reduction of the linearly reducible massless off-shell three-point graph $\Delta_{3,5}$ of figure 6 shows that

$$\Phi(\Delta_{3,5}) = \frac{\Gamma(2 + 3\varepsilon)}{p_1^{4+6\varepsilon}} \sum_{n=0}^{\infty} f_n \varepsilon^n \quad \text{with} \quad f_n \in L\left(\left\{0, 1, \bar{z}, \frac{1}{\bar{z}}\right\}\right)(z) \otimes L(\{0, 1\})(\bar{z}). \quad (\text{A.11})$$

Results for f_0 and f_1 are supplied (in this form) in the attached file.

References

- [1] O. V. Tarasov, *Connection between Feynman integrals having different values of the space-time dimension*, *Phys.Rev.* **D54** (1996) 6479–6490, [[hep-th/9606018](#)].
- [2] V. A. Smirnov, *Evaluating Feynman Integrals*, vol. 211 of *Springer Tracts in Modern Physics*. Springer, 2004.
- [3] C. Itzykson and J.-B. Zuber, *Quantum Field Theory*. Dover Publications, Inc., 2005.
- [4] C. Bogner and S. Weinzierl, *Feynman Graph Polynomials*, *International Journal of Modern Physics A* **25** (2010) 2585–2618, [[arXiv:1002.3458](#)].
- [5] F. C. S. Brown, *The Massless Higher-Loop Two-Point Function*, *Communications in Mathematical Physics* **287** (May, 2009) 925–958, [[arXiv:0804.1660](#)].
- [6] Maplesoft, a division of Waterloo Maple Inc., “Maple 16.”
- [7] C. Bogner and S. Weinzierl, *Resolution of singularities for multi-loop integrals*, *Comput.Phys.Commun.* **178** (2008) 596–610, [[arXiv:0709.4092](#)].
- [8] C. Bogner and F. C. S. Brown, *Symbolic integration and multiple polylogarithms*, *PoS LL2012* (2012) 053, [[arXiv:1209.6524](#)].
- [9] F. C. S. Brown, *On the periods of some Feynman integrals*, *ArXiv e-prints* (Oct., 2009) [[arXiv:0910.0114](#)].
- [10] E. Panzer, *On the analytic computation of massless propagators in dimensional regularization*, *Nuclear Physics B* **874** (Sept., 2013) 567–593, [[arXiv:1305.2161](#)].
- [11] J. Ablinger, J. Blümlein, A. Hasselhuhn, S. Klein, C. Schneider, and F. Wißbrock, *Massive 3-loop ladder diagrams for quarkonic local operator matrix elements*, *Nuclear Physics B* **864** (Nov., 2012) 52–84, [[arXiv:1206.2252](#)].
- [12] J. Blümlein, A. De Freitas, C. Raab, F. Wißbrock, J. Ablinger, A. Hasselhuhn, M. Round, C. Schneider, and A. von Manteuffel, *Recent Results on the 3-Loop Heavy Flavor Wilson Coefficients in Deep-Inelastic Scattering*, *ArXiv e-prints* (July, 2013) [[arXiv:1307.7548](#)].
- [13] J. Ablinger, J. Blümlein, A. De Freitas, A. Hasselhuhn, S. Klein, C. Schneider, and F. Wißbrock, *New Results on the 3-Loop Heavy Flavor Wilson Coefficients in Deep-Inelastic Scattering*, *ArXiv e-prints* (Jan., 2013) [[arXiv:1212.5950](#)].
- [14] S. Bloch and P. Vanhove, *The elliptic dilogarithm for the sunset graph*, *ArXiv e-prints* (Sept., 2013) [[arXiv:1309.5865](#)].

- [15] L. Adams, C. Bogner, and S. Weinzierl, *The two-loop sunrise graph with arbitrary masses*, *Journal of Mathematical Physics* **54** (May, 2013) 052303, [[arXiv:1302.7004](#)].
- [16] C. Bogner and M. Lüders, *Multiple polylogarithms and linearly reducible Feynman graphs*, *ArXiv e-prints* (Feb., 2013) [[arXiv:1302.6215](#)].
- [17] T. Gehrmann and E. Remiddi, *Differential equations for two loop four point functions*, *Nucl.Phys.* **B580** (2000) 485–518, [[hep-ph/9912329](#)].
- [18] J. M. Henn, A. V. Smirnov, and V. A. Smirnov, *Evaluating single-scale and/or non-planar diagrams by differential equations*, *ArXiv e-prints* (Dec., 2013) [[arXiv:1312.2588](#)].
- [19] J. M. Henn, A. V. Smirnov, and V. A. Smirnov, *Analytic results for planar three-loop four-point integrals from a Knizhnik-Zamolodchikov equation*, *JHEP* **1307** (2013) 128, [[arXiv:1306.2799](#)].
- [20] E. Remiddi and J. A. M. Vermaseren, *Harmonic polylogarithms*, *Int.J.Mod.Phys.* **A15** (2000) 725–754, [[hep-ph/9905237](#)].
- [21] A. V. Smirnov and M. N. Tentyukov, *Feynman Integral Evaluation by a Sector decomposition Approach (FIESTA)*, *Comput.Phys.Commun.* **180** (2009) 735–746, [[arXiv:0807.4129](#)].
- [22] F. Chavez and C. Duhr, *Three-mass triangle integrals and single-valued polylogarithms*, *Journal of High Energy Physics* **11** (Nov., 2012) 114, [[arXiv:1209.2722](#)].
- [23] F. C. S. Brown, *Polylogarithmes multiples uniformes en une variable*, *Comptes Rendus Mathematique* **338** (2004), no. 7 527–532.
- [24] O. Schnetz, *Graphical functions and single-valued multiple polylogarithms*, *ArXiv e-prints* (Feb., 2013) [[arXiv:1302.6445](#)].
- [25] J. Drummond, C. Duhr, B. Eden, P. Heslop, J. Pennington, and V. A. Smirnov, *Leading singularities and off-shell conformal integrals*, *Journal of High Energy Physics* **8** (Aug., 2013) 133, [[arXiv:1303.6909](#)].
- [26] T. Gehrmann, G. Heinrich, T. Huber, and C. Studerus, *Master integrals for massless three-loop form factors: One-loop and two-loop insertions*, *Physics Letters B* **640** (Sept., 2006) 252–259, [[hep-ph/0607185](#)].
- [27] G. Heinrich, T. Huber, D. A. Kosower, and V. A. Smirnov, *Nine-propagator master integrals for massless three-loop form factors*, *Physics Letters B* **678** (July, 2009) 359–366, [[arXiv:0902.3512](#)].
- [28] A. von Manteuffel and C. Studerus, *Massive planar and non-planar double box integrals for light N_f contributions to $gg \rightarrow t\bar{t}$* , *Journal of High Energy Physics* **10** (Oct., 2013) 37, [[arXiv:1306.3504](#)].
- [29] T. Gehrmann, L. Tancredi, and E. Weihs, *Two-loop master integrals for $q\bar{q} \rightarrow VV$: the planar topologies*, *Journal of High Energy Physics* **8** (Aug., 2013) 70, [[arXiv:1306.6344](#)].
- [30] J. M. Henn and V. A. Smirnov, *Analytic results for two-loop master integrals for Bhabha scattering I*, *JHEP* **1311** (2013) 041, [[arXiv:1307.4083](#)].
- [31] R. K. Ellis and G. Zanderighi, *Scalar one-loop integrals for QCD*, *Journal of High Energy Physics* **2** (Feb., 2008) 2, [[arXiv:0712.1851](#)].
- [32] J. Fleischer, F. Jegerlehner, and O. V. Tarasov, *A New hypergeometric representation of one loop scalar integrals in d dimensions*, *Nucl.Phys.* **B672** (2003) 303–328, [[hep-ph/0307113](#)].

- [33] J. C. Collins, *Renormalization*. Cambridge Monographs on Mathematical Physics. Cambridge University Press, 1984.
- [34] F. C. S. Brown and D. Kreimer, *Angles, scales and parametric renormalization*, *Letters in Mathematical Physics* **103** (2013), no. 9 933–1007, [[arXiv:1112.1180](#)].
- [35] T. Binoth and G. Heinrich, *An automatized algorithm to compute infrared divergent multiloop integrals*, *Nucl.Phys.* **B585** (2000) 741–759, [[hep-ph/0004013](#)].
- [36] T. Binoth and G. Heinrich, *Numerical evaluation of multiloop integrals by sector decomposition*, *Nucl.Phys.* **B680** (2004) 375–388, [[hep-ph/0305234](#)].
- [37] S. Borowka, J. Carter, and G. Heinrich, *Numerical Evaluation of Multi-Loop Integrals for Arbitrary Kinematics with SecDec 2.0*, *Comput.Phys.Commun.* **184** (2013) 396–408, [[arXiv:1204.4152](#)].
- [38] B. Jantzen, A. V. Smirnov, and V. A. Smirnov, *Expansion by regions: revealing potential and Glauber regions automatically*, *Eur.Phys.J.* **C72** (2012) 2139, [[arXiv:1206.0546](#)].
- [39] S. Weinberg, *High-energy behavior in quantum field theory*, *Phys. Rev.* **118** (May, 1960) 838–849.
- [40] E. R. Speer, *Ultraviolet and infrared singularity structure of generic Feynman amplitudes*, *Ann. Inst. H. Poincaré Sect. A (N.S.)* **23** (1975), no. 1 1–21.
- [41] F. C. S. Brown and K. A. Yeats, *Spanning Forest Polynomials and the Transcendental Weight of Feynman Graphs*, *Communications in Mathematical Physics* **301** (Jan., 2011) 357–382, [[arXiv:0910.5429](#)].
- [42] C. Duhr, H. Gangl, and J. R. Rhodes, *From polygons and symbols to polylogarithmic functions*, *Journal of High Energy Physics* **10** (Oct., 2012) 75, [[arXiv:1110.0458](#)].
- [43] C. Duhr, *Hopf algebras, coproducts and symbols: an application to Higgs boson amplitudes*, *JHEP* **2012** (2012), no. 8 043, [[arXiv:1203.0454](#)].
- [44] J. A. Lappo-Danilevsky, *Mémoires sur la théorie des systèmes des équations différentielles linéaires*, vol. I–III. Chelsea, 1953.